

# Binding Induced Stabilization Measured on the Same Molecular Protein Substrate using Single Molecule Magnetic Tweezers and Hetero-Covalent Attachments

Narayan Dahal, Joel Nowitzke, Annie Eis, Ionel Popa\*

Department of Physics, University of Wisconsin-Milwaukee, 3135 North Maryland Ave., Milwaukee, Wisconsin 53211, United States

**Correspondence:** \* Email: [popa@uwm.edu](mailto:popa@uwm.edu).

## ABSTRACT

Binding induced mechanical stabilization plays key roles in proteins involved in muscle contraction, cellular mechano transduction or bacterial adhesion. Due to the vector nature of force, single molecule force spectroscopy techniques are ideal for measuring the mechanical unfolding of proteins. However, current approaches are still prone to calibration errors between experiments, and geometrical variations between individual tethers. Here we introduce a single molecule assay based on magnetic tweezers and hetero-covalent attachment, which can measure the binding of substrate-ligand using the same protein molecule. We demonstrate this approach with protein L, a model bacterial protein which has two binding interfaces for the same region of kappa-light chain antibody ligands. Engineered molecules with eight identical domains of protein L between a HaloTag and a SpyTag were exposed to repeated unfolding-refolding cycles at forces up to 100 pN for several hours at a time. The unfolding behavior of the same protein was measured in solution buffers with different concentrations of antibody ligands. With increasing antibody concentration, an increasing number of protein L domains became more stable, indicative of ligand binding and mechanical reinforcement. Interestingly, the binding constant of the mechanically reinforced states coincides with that measured for the low-avidity binding interface of protein L, suggesting a physiological role for the second binding interface. The molecular approach presented here opens the road to a new type of binding experiments, where the same molecule can be exposed to different solvents or ligands.



## INTRODUCTION

Ligand binding can have a profound effect on the stability and function of a substrate protein. Several established methods use the co-localization between ligand and substrate to measure protein binding. Apart from being subject to false positives, these methods do not report on how binding affects the stability and function of the substrate proteins. Single molecule techniques can measure ligand binding as a change in the mechanical response to force<sup>1,2</sup>. A single molecule assay using the change in mechanical stability to measure ligand binding was first reported for NuG2 protein, which can bind its ligand without inducing structural changes<sup>3</sup>. While using statistics from different protein molecules pulled at constant speed, the authors demonstrated mechanical reinforcement upon ligand binding. Sugar ligand attaching to maltose-binding protein was also shown to induce a partitioning and change in the mechanical unfolding pathway via an unfolding intermediate<sup>4,5</sup>. Binding also plays key roles in proteins involved in mechano-transduction. Binding of vinculin to talin, the mechanical computer of cells, arrests this protein in an unfolded conformation and prevents refolding<sup>6,7</sup>. On the other extreme, binding of DLC-1, another talin partner, was predicted using computer simulations to not have any significant effect on the stability of its substrate<sup>8</sup>. Binding of small ions can also significantly affect the stability of a protein, with little structural changes<sup>9-11</sup>. For example, binding of copper ions to azurin, which does not affect the transition state, makes the protein-substrate unfold through different intermediates<sup>12,13</sup>.

Current single molecule force spectroscopy methods aiming to investigate binding-induced changes in the mechanical stability of a protein substrate rely on measuring many molecules in different experimental conditions. While these approaches produce important results, they can only be applied to substrates where ligand binding has a predictable effect. Effects such as protein aging<sup>14</sup>, misfolding<sup>15</sup>, or site-specific change in mechanical stability when there is more than one binding interface, are not easily accessible with these methods. Furthermore, several relative errors can be introduced when measuring different molecules, even using the same pre-calibrated force probe<sup>16</sup>. For example, both the tethering angle<sup>17</sup> and the size of the initial extension<sup>18</sup> can change from one tethered molecule to another.

Here, we demonstrate an approach based on covalent HaloTag and SpyTag attachment, which, combined with the stability of magnetic tweezers, allows the measurement of the same protein molecule for many unfolding/refolding cycles, at high forces and in the presence of various

concentrations of ligand. Using this hetero-covalent attachment, we investigate the mechanical response of the B1 domain of protein L (referred to from now on as simply protein L) in the presence of its known ligand,  $\kappa$ -light chain antibodies.

## METHODS

Unless otherwise specified, all chemicals were purchased from Sigma-Aldrich. Eight-repeats of protein L were inserted into a modified pFN18a vector (Promega), which introduces a HaloTag at the N-terminus and a SpyTag at the C-terminus. We chose to repeat protein L B1 domain eight times to produce better statistics and a unique fingerprint (of eight unfolding equal steps), and obtain good expression levels using bacterial expression system. Proteins diluted to  $\sim 100$  nM were left to adsorb on a functionalized SpyCatcher surface for  $\sim 30$  min, to allow for the maturation of the attachment through an isopeptide bond <sup>19</sup>. After washing the non-adsorbed proteins, paramagnetic beads (Thermo Fisher Scientific) with imbedded chloroalkane ligands (Promega) were left to react with the HaloTag end, which results in the formation of a covalent ester bond. Further details on protein engineering, expression and purification, and on surface and bead functionalization are provided in the SI.

The extension of single protein molecules at varying forces were obtained using the magnetic tweezers technique described in refs. <sup>20,21</sup>. In brief, the chamber was mounted on top of an inverted microscope (Olympus IX71), and the separation between the paramagnetic beads and a pair of permanent magnets was achieved using a voice-coil actuator (Equipment Solution). ROIs of 128x128 pixels were selected around a tethered super paramagnetic bead and a glued non-magnetic reference bead. At the beginning of each experiment, a stack library was obtained for the two selected beads by changing the focusing position with the help of a piezo actuator (P-725, PI) in equal steps of 20 nm. Two-dimensional fast Fourier transforms (2D-FFTs) of the ROI images were then used to obtain a radial profile as a function of focal distance for the two beads. During an experiment, the correlation between the radial profile of each bead was computed against its stack library and a Gaussian fit was used around the maximum of the correlation curve to determine the location of each bead. The extension of the molecule was measured as the difference between the position of the paramagnetic and reference beads. During measurements, any instrumental drift was also corrected by adjusting the position of the objective using the piezo actuator, such that the reference bead was maintained at the same focal point. All data acquisition and processing was

done in Igor Pro (WaveMetrics). Data analysis and errors estimation were done as explained in the SI section. The tethers considered in our analysis all had the expected unfolding fingerprint of eight unfolding steps of equal size. At least three different tethers were used for each data point.

## RESULTS

### A HaloTag-SpyTag approach for attachment of single proteins.

To measure the mechanical unfolding of proteins in the presence of their ligands, we introduce a combination of single molecule magnetic tweezers and covalent attachment. Eight repeats of protein L were engineered between a HaloTag at the N-terminus and a SpyTag at the C-terminus. We first test the binding efficiency of protein L to its antibody ligand and between SpyTag-SpyCatcher using a triple-developing approach (Figure 1). In this approach, we run two identical non-denaturing SDS-PAGE gels, where we load HaloTag-(protein L)8-SpyTag, GFP2-SpyCatcher, and the reaction mix between the two using two different concentrations (1 and 5  $\mu$ M). We then stain one gel with the regular Coomassie blue, and transfer the second to a cellulose membrane. The cellulose membrane is then exposed to an IgG mouse antibody solution, followed by incubation with a Horse Radish Peroxidase (HRP) secondary goat antimouse antibody. Under blue light, only the bands that have the native GFP2 protein show a signal (Figure 1B), while under Enhanced chemiluminescence (ECL) conditions, only bound antibodies produce signal (Figure 1C). This simple assay demonstrates that our construct successfully produces SpyTag-SpyCatcher attachment and that protein L binds specifically to kappa-light chain antibodies.

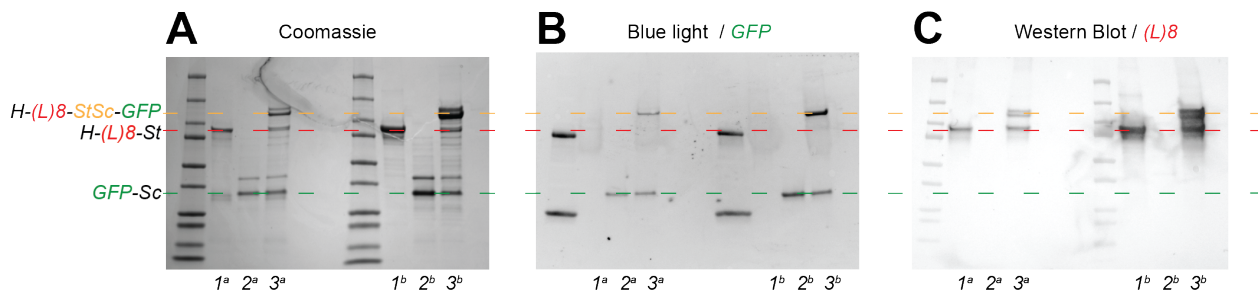


**Figure 1. Testing protein L – antibody binding and SpyTag-SpyCatcher chemistry.** A) SDS-PAGE gel having the molecular weight ladder followed by HaloTag-(protein L)8-SpyTag (denoted H-(L)8-St) in (1), GFP2-SpyCatcher (denoted GFP-Sc) in (2) and the mix of the two proteins in 1:1 molar ratio, in (3), loaded at two concentrations: 1  $\mu$ M in (a) and 5  $\mu$ M (b). The dotted lines represent the corresponding positions for GFP2-SpyCatcher (green), HaloTag-(protein L)8-SpyTag (red) and HaloTag-(protein L)8-SpyTag-SpyCatcher-GFP2 (orange). B) Same gel as in A after being transferred on a cellulose membrane, recorded under blue light with specific GFP filters. A new fluorescent band becomes apparent in (3), demonstrating the successful SpyTag-SpyCatcher reaction. (C) The same gel as in (B) was then incubated in mouse IgG antibodies (1  $\mu$ M) for 1 hour, and then developed with goat anti-mouse HRP fused secondary antibodies. This method demonstrates that mouse IgG antibodies are ligating protein L, in both unreacted and reacted SpyCatcher-SpyTag complex.

Magnetic tweezers can expose single protein molecules to forces in the pico-Newton range<sup>22,23</sup> for extensive periods of time, approaching several hours-per-molecule<sup>20</sup>, and can potentially sample many tethered beads simultaneously<sup>24,25</sup>. Force is applied through the separation between a pair of permanent magnets and a tethered paramagnetic bead and the extension is measured from the displacement of this bead in respect to a reference bead. An unfolding event registers as a nanometer step increase in the end-to-end protein length, where its size depends on the applied force and the number of amino acids inside the folded structure. To achieve these long tethering times, an active focus correction mechanism is used, where a non-magnetic reference bead glued to the glass surface is kept in focus by moving the objective vertically with the help of a piezo actuator. Covalent attachment is desirable, as it results in the most stable tethers and enable longer experiments at higher forces. Several specific covalent chemistries have been developed, based on HaloTag<sup>18,26</sup>, SpyTag<sup>19</sup>, cohesin-dockerin<sup>27,28</sup>, and click chemistry<sup>29,30</sup>. For our experiments here, we have engineered eight repeats of protein L sandwiched between a HaloTag at the N-terminus and a SpyTag at the C-terminus (Figure 2). While previously we used the Biotin-Streptavidin interaction to tether proteins through a C-terminus AviTag<sup>20</sup>, this noncovalent attachment becomes challenged when forces above ~60 pN are applied for over 1 minute<sup>31</sup> and could not have been used for the current experiment, where ligand binding increases the mechanical stability of protein L beyond this range. The breaking of the tether at high forces was solved here by using the SpyTag-SpyCatcher link, which can form a covalent isopeptide bond<sup>19</sup>. As opposed to the HaloTag-chloroalkane ligand interaction, which forms a covalent ester bond in under 1 second<sup>18</sup>, the isopeptide bond formation between SpyTag-SpyCatcher requires several minutes. Hence the glass surface was functionalized with SpyCatcher proteins before it was left to react with our C-terminated SpyTag protein L construct for 30 min (see Methods section for more details). Following a washing step, surface attached proteins were left to react for ~1 minute with the chloroalkane terminated superparamagnetic beads at the HaloTag site, before the magnets were brought down. This time is more than sufficient for the HaloTag interaction, and avoids non-specific or multiple tethers between the bead and the surface, which could form if longer times would be allowed for this step. When a force of 65 pN is applied to our protein L construct, we measure eight equidistant unfolding steps, unraveling in ~3 s (Figure 2C). The HaloTag-SpyTag attachment also allows us to change the solution buffer inside the fluid chamber without breaking

the molecular tether, and enabling the measurement of the same protein molecule in different concentrations of antibody. When we exchange the antibody-free solution buffer with one that contains  $\kappa$ -light chain antibodies and apply the same 65 pN force to the same molecule, we find that  $\sim$ 47 s are now needed to completely unfold all protein L domains (Figure 2C, blue trace). Hence, the antibody binding has a mechanical strengthening effect on protein L, and this effect can also be used to measure the binding of antibodies.

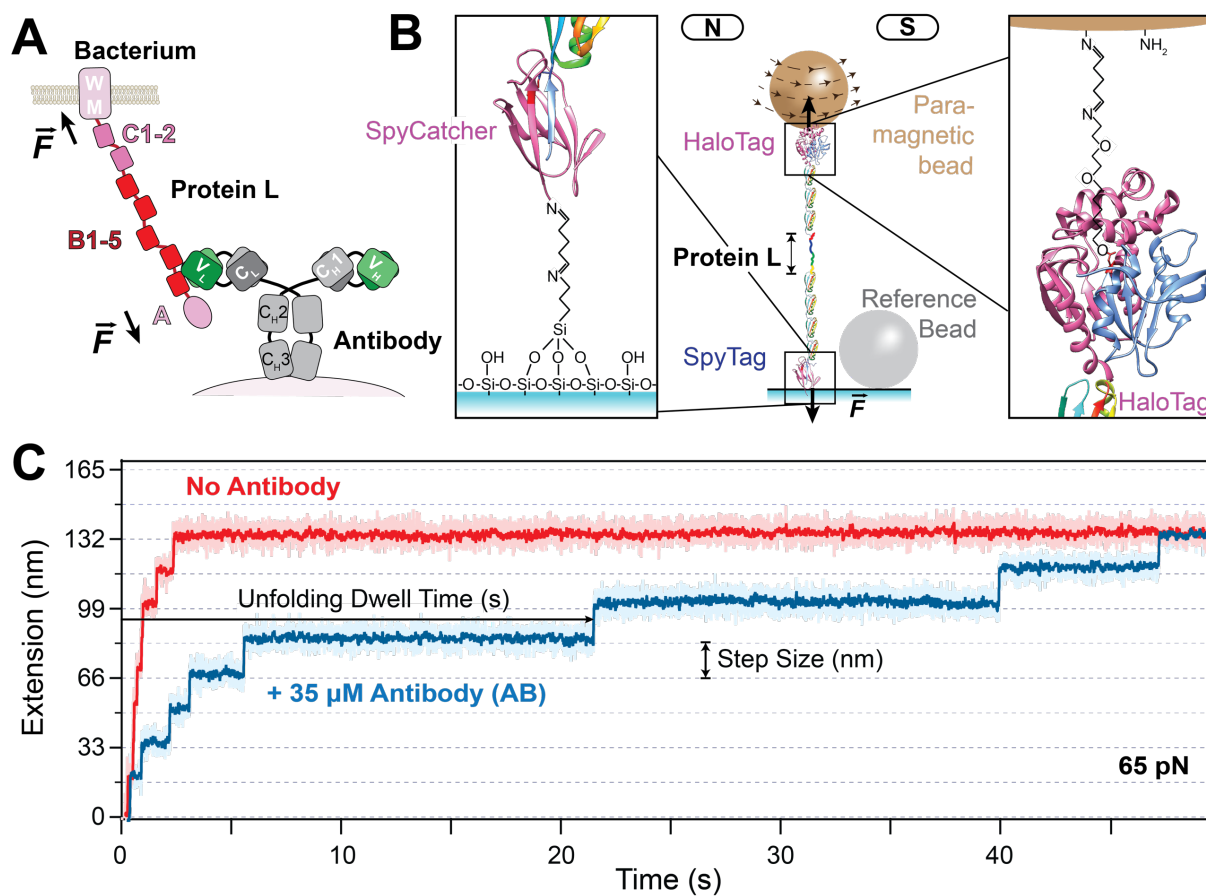


**Figure 2. Measurement of antibody binding to protein L using magnetic tweezers and HaloTag-SpyTag covalent attachments.** A) Schematics of attachment of a multidomain protein L (top) secreted by *Finegoldia magna* (formerly *Peptostreptococcus magnus*), which secretes protein L as a chain of several domains: a wall domain W, a membrane bound domain M, several C domains (varying depending on the strain), five B domains and one A domain. All B domains have developed binding affinity to antibodies at the  $\kappa$ -light chain site and have the residues involved in antibody binding conserved<sup>32</sup>. B) Schematics of the tethered polyprotein engineered with a SpyTag and a HaloTag. Inset left: attachment chemistry used for the SpyCatcher/SpyTag reaction to attach the protein to the glass coverslip. Inset right: attachment chemistry used for the chloroalkane-ligand/HaloTag reaction to attach the protein to the amine-terminated paramagnetic bead. C) Example of a trace of the same single molecule unfolding all its eight domains in

the absence (red) and presence (blue) of antibodies (35  $\mu$ M) under a constant force (65 pN). Each step corresponds to the unfolding and extension of a protein L domain. The unfolding dwell-time and step size are defined as indicated by the arrows, with the zero value for both at the time/length set just after the change in force.

### Using mechanical unfolding to measure antibody binding

To measure the binding interaction between protein L and IgG antibodies, we use a two-step force pulse protocol, which allows us to determine how many domains have a ligand attached to them (Figure 3). First, the force is ramped to a low-force (45 pN) and maintained at this value for a total of 35 s. At this force, the unfolding rate of protein L is  $0.25 \pm 0.01 \text{ s}^{-1}$  – it takes on average  $\sim 4$  s dwell time to unfold a domain. This exposure time is generally sufficient to unfold all the protein L domains free of antibodies. We then ramp the force once more and maintain it at 100 pN for 100 s. This second high-force pulse is used to determine the number of protein L domains with bound antibodies. Indeed, without any antibodies added, protein L unfolds all its eight domains in the first low-force pulse (45 pN, Figure 3A). When (protein L)<sub>8</sub> is measured in a solution containing 35  $\mu$ M antibodies, most of the unfolding events appear in the high-force pulse (100 pN, Figure 3B). At the end of each 100 s – 100 pN exposure, the protein is left to refold at  $\sim 2$  pN for 100 s and bind new antibody molecules from solution. As we can tether single protein L molecules for extensive time and expose them to alternating high and low force pulses, we are effectively resetting the binding process with every cycle. We then quantify the binding as the number of unfolding domains in the 100 pN region over the total number of domains (the last bar in Figure 3C). In 35  $\mu$ M IgG,  $\sim 75\%$  of the unfolding events appear in the high-force 100 pN pulse (Figure 3C).

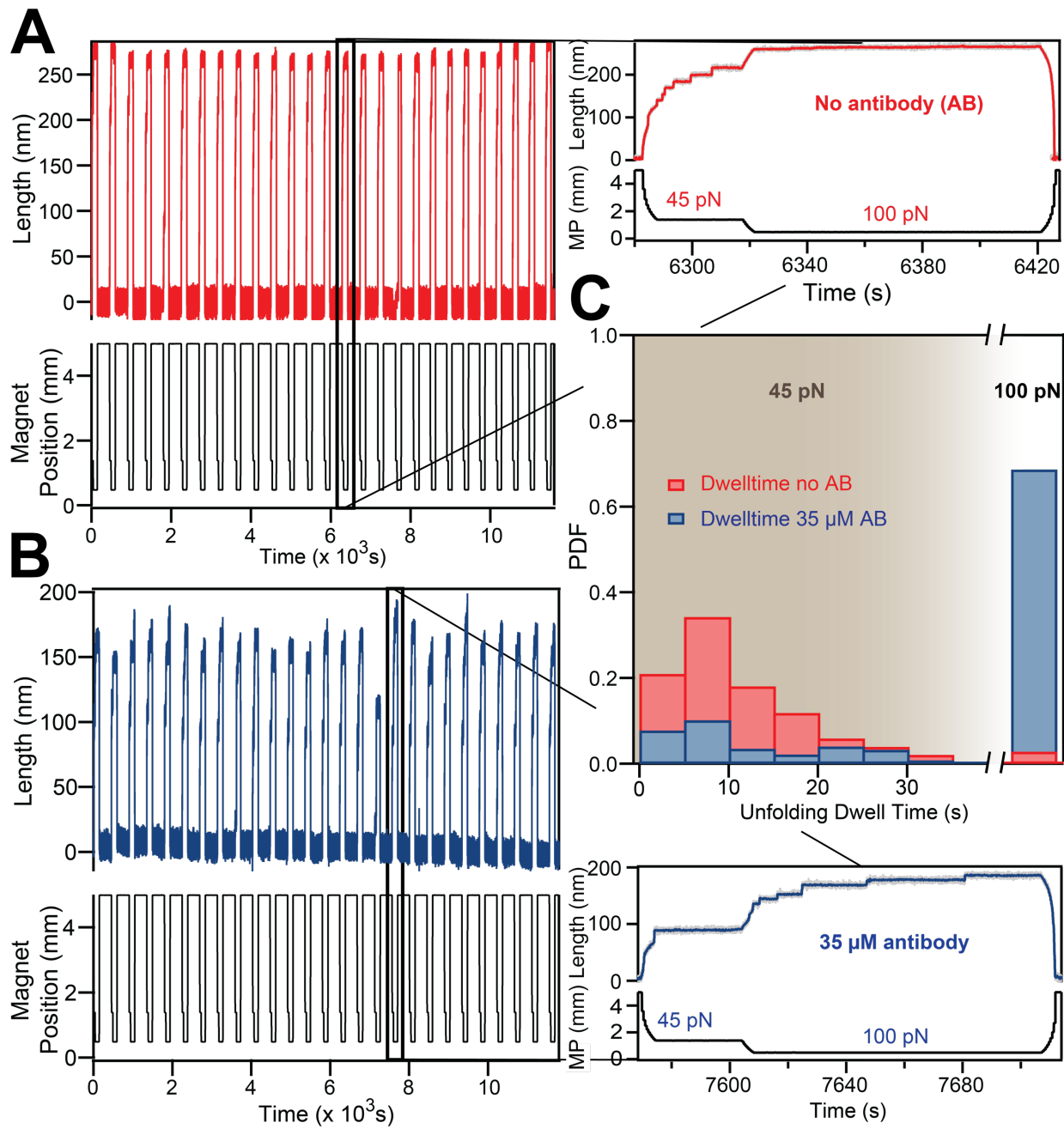


**Figure 3. Measurement of antibody binding using a two-step protocol.** A) Representative unfolding trace of octamer of protein L domain in the absence of antibody. The force protocol was set to 45 pN for  $\sim$ 35 seconds, followed by ramping the force to 100 pN. Zoom in (Top right) shows the unfolding of all 8 domains within 30 seconds at 45 pN. B) Similar unfolding trace obtained from the same construct with same force protocol measured in the presence of 35  $\mu$ M mouse serum IgG. Zoom in (Bottom right) shows the unfolding of the majority of protein domains at high force (100 pN) in the presence of antibody. C) Probability distribution function (PDF) of the unfolding dwell time frequency histograms of protein L domains in absence and in presence of 35  $\mu$ M IgG. In absence of IgG, more than

90% of domains unfold within 35 seconds at the low pulling force of 45 pN (red histogram) whereas in the presence of 35  $\mu$ M IgG, most of the domains unfold in the high force pulse of 100 pN (blue histogram).

By repeating the two-pulse protocol with changing antibody concentrations, we can determine the binding constant to protein L (Figure 4A). As the antibody concentration is increased, more and more unfolding events appear in the 100 pN region of the pulse. However, the binding probability plateaus at a value of  $\sim 0.75$  at concentrations above 30  $\mu$ M (Figure 4B). Even at the lowest added antibody concentration, the number of ligand molecules in solution is orders of magnitude higher than the number of adsorbed protein L molecules. Hence the added antibody concentration equals the equilibrium concentration. The fitted dissociation constant between the IgG antibodies and protein L, using the Hill-Langmuir equation  $X_{AB-L} = [AB]/(K_D + [AB])$ , has a value of  $23 \pm 3$   $\mu$ M. The measured binding constant is smaller than that reported from titration experiments, which was 0.1-0.2  $\mu$ M <sup>33</sup>. The same authors reported that treatment with tetrinitromethane, which is a tyrosine inhibitor, prevents normal antibody binding at the  $\beta 1$ - $\beta 2$ - $\alpha$  interface, and decreases the binding constant to  $\sim 30$   $\mu$ M <sup>33</sup>. This change in binding affinity was later explained by the discovery of a second binding interface at the  $\alpha$ - $\beta 3$  site <sup>34</sup>. The measured value here for the binding constant via mechanical unfolding suggests that it is this second interface that plays a role in mechanosensing.

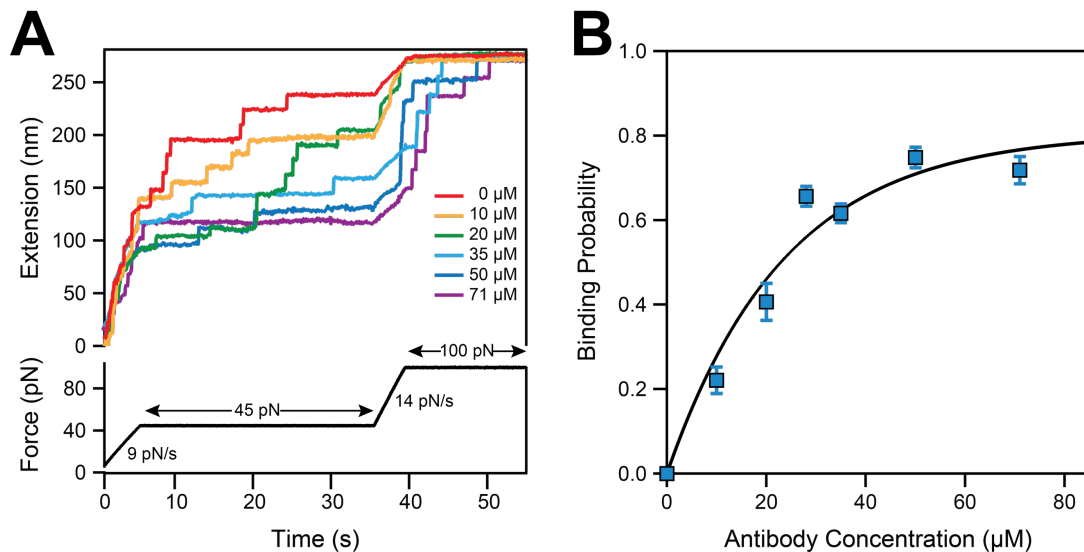


**Figure 4. Determining the dissociation constant from the change in the mechanical stability of protein L.** A) Unfolding traces of protein L octamer from the HaloTag-(protein L)<sub>8</sub>-SpyTag construct, measured in different

concentration of mouse IgG antibody. Without antibody, all the domains unfold at low force (45 pN, red trace) whereas a high concentration of antibody requires a high force (100 pN, violet trace, 71  $\mu$ M antibody) to unfold. B) The binding probability as a function of the concentration of IgG. Increasing the concentration of antibody increases the binding probability and thus the stability. Blue squares represent the binding probability at different concentration of antibody. The line represents a fit using Hill-Langmuir equation and yielding a dissociation constant  $K_D = 23 \pm 3 \mu$ M. Error bars are S.E. obtained via bootstrapping.

### Antibody-binding induces a pseudo catch-bond behavior

Not only does our single molecule assay constitute an elegant approach to measure antibody binding, but it can also determine the unfolding kinetics of protein L in the presence and absence of its IgG ligand. The dwell time distributions describing the collective behaviors of protein domains were scaled to a single protein L - antibody ligand interaction <sup>35,36</sup>. For measuring unfolding kinetics, we use the square-root histogram method <sup>37,38</sup> (histogram of logarithmic binning of the unfolding dwell time – see Figure 5A and B, and Figure S1). In this case, the protein L octamer construct was exposed to a single constant force in the absence and presence of antibodies at a saturating concentration (see also Figure 4B). The dwell time for unfolding was determined as a function of force and experimental conditions, as defined in Figure 2C. Histograms were then constructed from the natural logarithm of the measured dwell-times and fitted to a single-exponential law:  $\exp[x - x_0 - \exp(x - x_0)]$  when a single peak was present, and a double exponential law:  $A_1 \exp[x_1 - x_{01} - \exp(x_1 - x_{01})] + A_2 \exp[x_2 - x_{02} - \exp(x_2 - x_{02})]$  when the histogram had two peaks (with  $x = \ln[t]$ ,  $x_0 = -\ln[r(F)]$  where  $t$  is the unfolding dwell time and  $r(F)$  is the force-dependent unfolding rate. The square-root histogram method has the advantage of separating processes taking place on different characteristic timescales. The distribution of unfolding events at low forces exhibited a bimodal shape with ~ 10-20 % of the events in a weak state (black points in Figure 5C) and the remaining in a more mechanically stable state. This behavior was attributed to ephemeral states and domain swapping in a previous study <sup>38</sup>. As the experienced force is increased, the histogram peak of the unfolding dwell times moves to lower dwell-time values and the first peak is no longer present (compare red histograms in Figures 5A and B). The unfolding kinetics measured here for protein L in the absence of antibody is similar to that measured for the same protein using different attachment chemistry <sup>38</sup>.

The square-root histogram method is very useful at high forces (>40 pN) for separating the unfolding events of protein L arising from domains that have bound antibodies from the ones that

do not (Figure 5B). In this case, we first use the antibody-free experiments to determine the unfolding rates at a given force (red histogram Figure 5B). We then fit a double exponential law to measure the unfolding kinetics of antibody-bound protein L domains (blue histogram Figure 5B). To describe the unfolding rates as a function of force, we then use the Bell model  $\ln[r(F)] = \ln[r_0] + \frac{F \cdot \Delta x}{kT}$  (Figure 5C), where  $r_0$  is the extrapolated rate at zero force,  $F$  is the applied force,  $\Delta x$  is the distance to transition state and  $kT$  the Boltzmann thermal energy. An interesting finding is that the unfolding rate of the protein L domains with bound antibodies has a different dependency slope with force than the unfolding rate of the protein L free of antibody (blue vs red points in Figure 5C). These dependencies are characterized by a distance to transition state of  $0.24 \pm 0.04$  nm for protein L with bound antibody and  $0.42 \pm 0.01$  nm for protein L without bound antibodies, and suggests that the higher the experienced force, the larger the mechanical stabilization effect is.

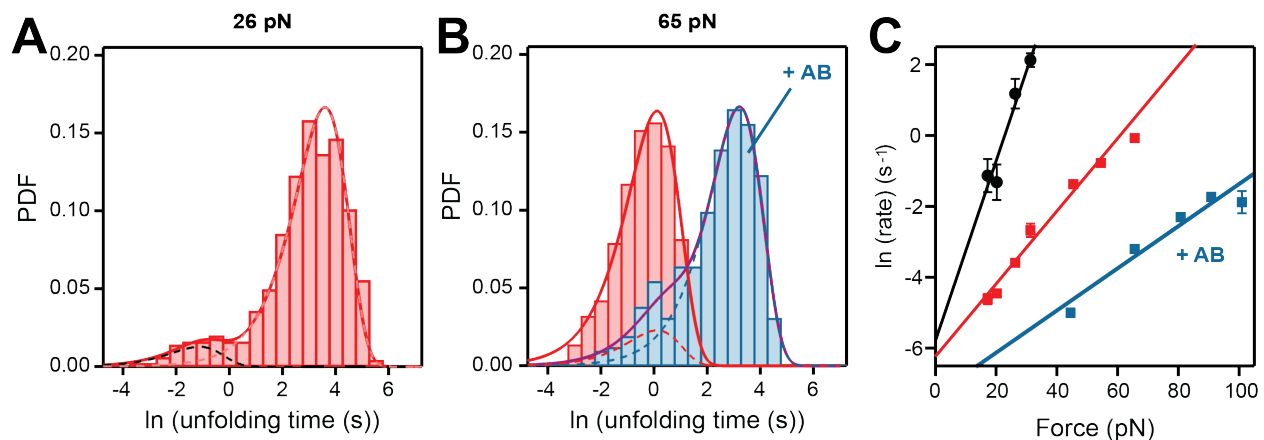


**Figure 5. Force-dependent unfolding kinetics of protein L in the presence and absence of antibodies.** A) Histogram of the natural logarithm of the measured dwell-times of protein L without added antibodies, at 26 pN. The dotted lines represent the individual fits using a single exponential law, while the continuous line is their sum. Between 10-20% of protein L domains are measured in a mechanically weak state, a number similar to the percentage of domains that do not bind antibodies, but a direct correlation between the two populations cannot be readily made. This weak state was previously attributed to domain swapping<sup>38,39</sup>. B) Histogram of the natural logarithm of the measured dwell-times of protein L at 65 pN without antibodies (red) and in the presence of antibodies (35  $\mu$ M, blue). The first peak in the blue histogram coincides with the location of the red peak and has an amplitude that corresponds to  $\sim 12\%$  unbound domains, in agreement with the experiments from the double-pulse protocol (Figure 4). C) Unfolding rates of the weak state of protein L (black circles), of the native state (red squares), and antibody-bound state (blue squares). The lines represent the fits using the Bell's model. Error bars are S.E. obtained via bootstrapping.

## DISCUSSION

The state of the art in using single molecule resolution to investigate a biophysical process currently entails repeating the desired experiment on many molecules, in diverse experimental conditions. With the advent of magnetic tweezers and covalent attachment via HaloTag, we have managed to extend the sampling time for a single molecule from several minutes to 15 days<sup>20</sup>. However, this approach was using the weaker non-covalent biotin-Streptavidin interaction, limiting the force exposure to relatively low values. By introducing a second SpyTag covalent attachment via an isopeptide bond<sup>19</sup>, we can now increase the force-exposure time range and titrate binding at single molecular level. We demonstrate this approach with a protein L construct, which has HaloTag at the N-terminus and SpyTag at the C-terminus. Protein L is one of several bacterial pathogens that secrete surface proteins that bind antibodies in order to protect themselves from the adaptive immune response and have evolved to operate under the mechanical sheer generated by mucus flow, coughing or urination <sup>40</sup> and must withstand mechanical stress to prevent being removed by fluid flow <sup>41-43</sup>. All protein L domains have two antibody-binding sites with vastly different avidity and the function of the second weaker binding interface is currently unknown <sup>33,34,44</sup>.

Our results here demonstrate that antibody binding increases the mechanical stability of protein L, and this increase is due to the binding at the second (low avidity) binding site (Figure 6). *In vivo*, the high-avidity binding site must be used to engage the tether, while the low-avidity binding site acts as a mechano-sensor, allowing bacteria to sample the antibody surface concentration and localize its search during successful binding under strain. In this way, the bacterium can fine tune its search radii under force, based on the surface concentration of exposed antibodies. It is well-known that antibodies form transient clusters on the membrane of dendritic cells, when acting as docking sites for the complement system or phagocytes <sup>45</sup>. When the bacterium attaches to its substrate, if the antibody surface concentration is low, the high-avidity binding site is more likely to engage, without influencing the mechanical stability of protein L. In this case, the anchored bacteria can unfold and extend its domains and increase its search radius. When interacting with an antibody cluster, some protein L domains can bridge two antibody

molecules at their light-chain region, increasing their mechanical stability and acting as force-sensors. Under flow, when the bacterium engages an antibody cluster, its search radius reduces from  $\sim 19$  nm/domain to  $\sim 4$  nm/domain <sup>21</sup>. This reduction in the search radius would allow the bacterium to counteract an immune response. We postulate that, while the first binding site acts as an attachment ligand due to its high avidity, it is the second binding site that can engage under flow and produce a mechanical signal, informing on the concentration of the antibodies at the target site. We propose that this mechano-sensor constitutes a rather unique mechanism through which bacteria can tune their search radius under force and orient the secreted protein L chains toward either a fight or flight mechanism.

Protein unfolding *in vivo* was previously correlated with exposure of cryptic sites, that can result in force-triggered redox reactions <sup>46,47</sup> or activated binding <sup>2,6</sup>. Furthermore, several bacteria were shown to have evolved internal isopeptide <sup>48,49</sup>, disulfide <sup>50,51</sup> or thioester bonds <sup>52-54</sup>, that prevent mechanical unfolding, which can lead to proteolysis. Our experiments demonstrate that we can now titrate these interactions and measure the change of the mechanical response of a single protein molecule, by using magnetic tweezers and hetero-covalent attachment. This approach will not only prove important for discovering mechanical effects related to ligand binding, as we show here, but also opens the road to screening of mechano-active compounds with single molecular resolution.

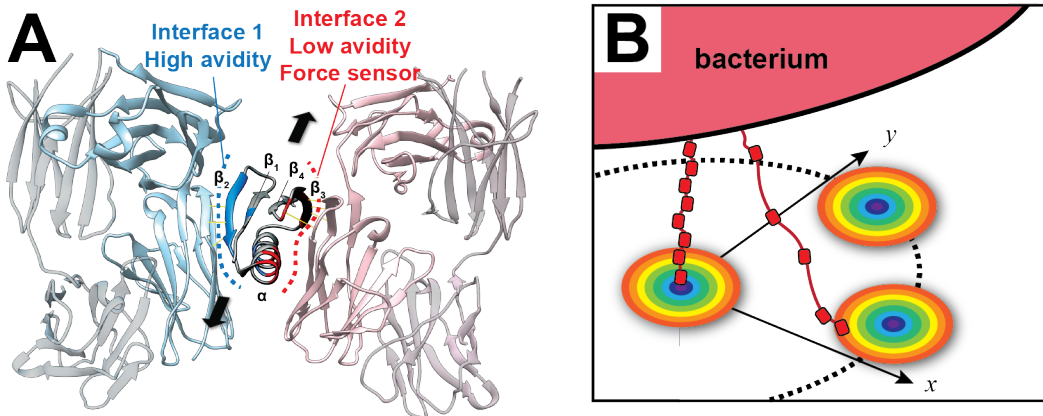


**Figure 6. Double-binding interface of protein L to its antibody ligand.** A) Ribbon representation of protein L bound to two antibody molecules. The high-avidity interface is shown in blue, while the low-avidity interface, which can act as a force-sensor, is drawn with red (based on PDB: 1HEZ <sup>34</sup>). The arrows show the direction of the force vector. B) Proposed mechanism, where the bacterium secretes protein L multidomains to attach to antibodies. The

circles denote the antibody clusters present at the cell surface<sup>45</sup>. High antibody concentrations will lock protein L in a folded conformation by populating both interfaces, reducing the search radius. Low antibody concentration will allow attachment at the high-avidity interface, without affecting the mechanical stability and increasing the search radius.

## ASSOCIATED CONTENT

### Supporting Information

Supporting Information is available in SI file.

## ACKNOWLEDGEMENTS

We acknowledge Mr. Benjamin Delebreau for help with measurements and all members of the Popa lab for useful discussions. This research was funded by the National Science Foundation (grant number MCB-1846143 and DBI-1919670), by the Greater Milwaukee Foundation (Shaw Award), the University of Wisconsin system (RGI 101X396).

## REFERENCES

- 1 Wiita, A. P., Perez-Jimenez, R., Walther, K. A., Grater, F., Berne, B. J., Holmgren, A., Sanchez-Ruiz, J. M. & Fernandez, J. M. Probing the chemistry of thioredoxin catalysis with force. *Nature* **450**, 124, (2007).
- 2 Yao, M., Qiu, W., Liu, R., Efremov, A. K., Cong, P., Seddiki, R., Payre, M., Lim, C. T., Ladoux, B., Mege, R. M. & Yan, J. Force-dependent conformational switch of alpha-catenin controls vinculin binding. *Nat Commun* **5**, 4525, (2014).
- 3 Cao, Y., Balamurali, M. M., Sharma, D. & Li, H. A functional single-molecule binding assay via force spectroscopy. *Proc Natl Acad Sci U S A* **104**, 15677-15681, (2007).
- 4 Aggarwal, V., Kulothungan, S. R., Balamurali, M. M., Saranya, S. R., Varadarajan, R. & Ainavarapu, S. R. Ligand-modulated parallel mechanical unfolding pathways of maltose-binding proteins. *J Biol Chem* **286**, 28056-28065, (2011).
- 5 Bertz, M. & Rief, M. Ligand binding mechanics of maltose binding protein. *J Mol Biol* **393**, 1097-1105, (2009).
- 6 del Rio, A., Perez-Jimenez, R., Liu, R., Roca-Cusachs, P., Fernandez, J. M. & Sheetz, M. P. Stretching single talin rod molecules activates vinculin binding. *Science* **323**, 638-641, (2009).

7 Margadant, F., Chew, L. L., Hu, X., Yu, H., Bate, N., Zhang, X. & Sheetz, M. Mechanotransduction in vivo by repeated talin stretch-relaxation events depends upon vinculin. *PLoS Biol* **9**, e1001223, (2011).

8 Haining, A. W. M., Rahikainen, R., Cortes, E., Lachowski, D., Rice, A., von Essen, M., Hytonen, V. P. & Del Rio Hernandez, A. Mechanotransduction in talin through the interaction of the R8 domain with DLC1. *PLoS Biol* **16**, e2005599, (2018).

9 Shen, T., Cao, Y., Zhuang, S. & Li, H. Engineered bi-histidine metal chelation sites map the structure of the mechanical unfolding transition state of an elastomeric protein domain GB1. *Biophys J* **103**, 807-816, (2012).

10 Ge, L., Perez, C., Waclawska, I., Ziegler, C. & Muller, D. J. Locating an extracellular K+-dependent interaction site that modulates betaine-binding of the Na+-coupled betaine symporter BetP. *Proc Natl Acad Sci U S A* **108**, E890-898, (2011).

11 Ramanujam, V., Kotamarthi, H. C. & Ainavarapu, S. R. Ca<sup>2+</sup> binding enhanced mechanical stability of an archaeal crystallin. *PLoS One* **9**, e94513, (2014).

12 Beedle, A. E. M., Lezamiz, A., Stirnemann, G. & Garcia-Manyes, S. The mechanochemistry of copper reports on the directionality of unfolding in model cupredoxin proteins. *Nat Commun* **6**, 7894, (2015).

13 Yadav, A., Paul, S., Venkatramani, R. & Ainavarapu, S. R. K. Differences in the mechanical unfolding pathways of apo- and copper-bound azurins. *Sci Rep* **8**, 1989, (2018).

14 Valle-Orero, J., Rivas-Pardo, J. A., Tapia-Rojo, R., Popa, I., Echelman, D. J., Haldar, S. & Fernandez, J. M. Mechanical Deformation Accelerates Protein Ageing. *Angew Chem Int Ed Engl* **56**, 9741-9746, (2017).

15 Marinko, J. T., Huang, H., Penn, W. D., Capra, J. A., Schlebach, J. P. & Sanders, C. R. Folding and Misfolding of Human Membrane Proteins in Health and Disease: From Single Molecules to Cellular Proteostasis. *Chem Rev* **119**, 5537-5606, (2019).

16 Pimenta-Lopes, C., Suay-Corredera, C., Velazquez-Carreras, D., Sanchez-Ortiz, D. & Alegre-Cebollada, J. Concurrent atomic force spectroscopy. *Communications Physics* **2**, (2019).

17 Carrion-Vazquez, M., Oberhauser, A. F., Fisher, T. E., Marszalek, P. E., Li, H. & Fernandez, J. M. Mechanical design of proteins studied by single-molecule force spectroscopy and protein engineering. *Prog Biophys Mol Biol* **74**, 63-91, (2000).

18 Popa, I., Berkovich, R., Alegre-Cebollada, J., Badilla, C. L., Rivas-Pardo, J. A., Taniguchi, Y., Kawakami, M. & Fernandez, J. M. Nanomechanics of HaloTag tethers. *J Am Chem Soc* **135**, 12762-12771, (2013).

19 Zakeri, B., Fierer, J. O., Celik, E., Chittcock, E. C., Schwarz-Linek, U., Moy, V. T. & Howarth, M. Peptide tag forming a rapid covalent bond to a protein, through engineering a bacterial adhesin. *Proc Natl Acad Sci U S A* **109**, E690-697, (2012).

20 Popa, I., Rivas-Pardo, J. A., Eckels, E. C., Echelman, D. J., Badilla, C. L., Valle-Orero, J. & Fernandez, J. M. A HaloTag Anchored Ruler for Week-Long Studies of Protein Dynamics. *J Am Chem Soc* **138**, 10546-10553, (2016).

21 Valle-Orero, J., Rivas-Pardo, J. A. & Popa, I. Multidomain proteins under force. *Nanotechnology* **28**, 174003, (2017).

22 Neuman, K. C. & Nagy, A. Single-molecule force spectroscopy: optical tweezers, magnetic tweezers and atomic force microscopy. *Nat Methods* **5**, 491-505, (2008).

23 Chen, H., Fu, H., Zhu, X., Cong, P., Nakamura, F. & Yan, J. Improved high-force magnetic tweezers for stretching and refolding of proteins and short DNA. *Biophys J* **100**, 517-523, (2011).

24 Lof, A., Walker, P. U., Sedlak, S. M., Gruber, S., Obser, T., Brehm, M. A., Benoit, M. & Lipfert, J. Multiplexed protein force spectroscopy reveals equilibrium protein folding dynamics and the low-force response of von Willebrand factor. *Proc Natl Acad Sci U S A* **116**, 18798-18807, (2019).

25 De Vlaminck, I., Henighan, T., van Loenhout, M. T., Burnham, D. R. & Dekker, C. Magnetic forces and DNA mechanics in multiplexed magnetic tweezers. *PLoS One* **7**, e41432, (2012).

26 Popa, I., Kosuri, P., Alegre-Cebollada, J., Garcia-Manyes, S. & Fernandez, J. M. Force dependency of biochemical reactions measured by single-molecule force-clamp spectroscopy. *Nat Protoc* **8**, 1261-1276, (2013).

27 Stahl, S. W., Nash, M. A., Fried, D. B., Slutski, M., Barak, Y., Bayer, E. A. & Gaub, H. E. Single-molecule dissection of the high-affinity cohesin-dockerin complex. *Proc Natl Acad Sci U S A* **109**, 20431-20436, (2012).

28 Milles, L. F., Schulten, K., Gaub, H. E. & Bernardi, R. C. Molecular mechanism of extreme mechanostability in a pathogen adhesin. *Science* **359**, 1527-1533, (2018).

29 Walder, R., LeBlanc, M. A., Van Patten, W. J., Edwards, D. T., Greenberg, J. A., Adhikari, A., Okoniewski, S. R., Sullan, R. M. A., Rabuka, D., Sousa, M. C. & Perkins, T. T. Rapid Characterization of a Mechanically Labile alpha-Helical Protein Enabled by Efficient Site-Specific Bioconjugation. *J Am Chem Soc* **139**, 9867-9875, (2017).

30 Ta, D. T., Vanella, R. & Nash, M. A. Bioorthogonal Elastin-like Polypeptide Scaffolds for Immunoassay Enhancement. *ACS Appl Mater Interfaces* **10**, 30147-30154, (2018).

31 Sedlak, S. M., Schendel, L. C., Melo, M. C. R., Pippig, D. A., Luthey-Schulthen, Z., Gaub, H. E. & Bernardi, R. C. Direction Matters: Monovalent Streptavidin/Biotin Complex under Load. *Nano Lett* **19**, 3415-3421, (2019).

32 Wikstrom, M., Drakenberg, T., Forsen, S., Sjoberg, U. & Bjorck, L. Three-dimensional solution structure of an immunoglobulin light chain-binding domain of protein L. Comparison with the IgG-binding domains of protein G. *Biochemistry* **33**, 14011-14017, (1994).

33 Beckingham, J. A., Housden, N. G., Muir, N. M., Bottomley, S. P. & Gore, M. G. Studies on a single immunoglobulin-binding domain of protein L from *Peptostreptococcus magnus*: the role of tyrosine-53 in the reaction with human IgG. *Biochem J* **353**, 395-401, (2001).

34 Graille, M., Stura, E. A., Housden, N. G., Beckingham, J. A., Bottomley, S. P., Beale, D., Taussig, M. J., Sutton, B. J., Gore, M. G. & Charbonnier, J. B. Complex between *Peptostreptococcus magnus* protein L and a human antibody reveals structural convergence in the interaction modes of Fab binding proteins. *Structure* **9**, 679-687, (2001).

35 Lei, H., He, C., Hu, C., Li, J., Hu, X., Hu, X. & Li, H. Single-Molecule Force Spectroscopy Trajectories of a Single Protein and Its Polyproteins Are Equivalent: A Direct Experimental Validation Based on A Small Protein NuG2. *Angew Chem Int Ed Engl* **56**, 6117-6121, (2017).

36 Garcia-Manyes, S., Brujic, J., Badilla, C. L. & Fernandez, J. M. Force-clamp spectroscopy of single-protein monomers reveals the individual unfolding and folding pathways of I27 and ubiquitin. *Biophys J* **93**, 2436-2446, (2007).

37 Sigworth, F. J. & Sine, S. M. Data transformations for improved display and fitting of single-channel dwell time histograms. *Biophys J* **52**, 1047-1054, (1987).

38 Tapia-Rojo, R., Eckels, E. C. & Fernandez, J. M. Ephemeral states in protein folding under force captured with a magnetic tweezers design. *Proc Natl Acad Sci U S A* **116**, 7873-7878, (2019).

39 O'Neill, J. W., Kim, D. E., Johnsen, K., Baker, D. & Zhang, K. Y. Single-site mutations induce 3D domain swapping in the B1 domain of protein L from *Peptostreptococcus magnus*. *Structure* **9**, 1017-1027, (2001).

40 Boyanova, L., Markovska, R. & Mitov, I. Virulence arsenal of the most pathogenic species among the Gram-positive anaerobic cocci, *Finegoldia magna*. *Anaerobe* **42**, 145-151, (2016).

41 Otto, M. Physical stress and bacterial colonization. *FEMS Microbiol Rev* **38**, 1250-1270, (2014).

42 Biais, N., Ladoux, B., Higashi, D., So, M. & Sheetz, M. Cooperative retraction of bundled type IV pili enables nanonewton force generation. *PLoS Biol* **6**, e87, (2008).

43 Thomas, W. E., Trintchina, E., Forero, M., Vogel, V. & Sokurenko, E. V. Bacterial adhesion to target cells enhanced by shear force. *Cell* **109**, 913-923, (2002).

44 Housden, N. G., Harrison, S., Roberts, S. E., Beckingham, J. A., Graille, M., Stura, E. & Gore, M. G. Immunoglobulin-binding domains: Protein L from *Peptostreptococcus magnus*. *Biochem Soc Trans* **31**, 716-718, (2003).

45 Preiner, J., Kodera, N., Tang, J., Ebner, A., Brameshuber, M., Blaas, D., Gelbmann, N., Gruber, H. J., Ando, T. & Hinterdorfer, P. IgGs are made for walking on bacterial and viral surfaces. *Nat Commun* **5**, 4394, (2014).

46 Alegre-Cebollada, J., Kosuri, P., Giganti, D., Eckels, E., Rivas-Pardo, J. A., Hamdani, N., Warren, C. M., Solaro, R. J., Linke, W. A. & Fernandez, J. M. S-Glutathionylation of Cryptic Cysteines Enhances Titin Elasticity by Blocking Protein Folding. *Cell* **156**, 1235-1246, (2014).

47 Beedle, A. E. M., Mora, M., Lynham, S., Stirnemann, G. & Garcia-Manyes, S. Tailoring protein nanomechanics with chemical reactivity. *Nat Commun* **8**, 15658, (2017).

48 Hendrickx, A. P. A., Budzik, J. M., Oh, S. Y. & Schneewind, O. Architects at the bacterial surface - sortases and the assembly of pili with isopeptide bonds. *Nature Reviews Microbiology* **9**, 166-176, (2011).

49 Alonso-Caballero, A., Schonfelder, J., Poly, S., Corsetti, F., De Sancho, D., Artacho, E. & Perez-Jimenez, R. Mechanical architecture and folding of *E. coli* type 1 pilus domains. *Nat Commun* **9**, 2758, (2018).

50 Reardon-Robinson, M. E. & Ton-That, H. Disulfide-Bond-Forming Pathways in Gram-Positive Bacteria. *J Bacteriol* **198**, 746-754, (2015).

51 Manteca, A., Alonso-Caballero, A., Fertin, M., Poly, S., De Sancho, D. & Perez-Jimenez, R. The influence of disulfide bonds on the mechanical stability of proteins is context dependent. *Journal of Biological Chemistry* **292**, 13374-13380, (2017).

52 Wong, S. G. & Dessen, A. Structure of a bacterial alpha2-macroglobulin reveals mimicry of eukaryotic innate immunity. *Nat Commun* **5**, 4917, (2014).

53 Walden, M., Edwards, J. M., Dziewulska, A. M., Bergmann, R., Saalbach, G., Kan, S. Y., Miller, O. K., Weckener, M., Jackson, R. J., Shirran, S. L., Botting, C. H., Florence, G. J., Rohde, M., Banfield, M. J. & Schwarz-Linek, U. An internal thioester in a pathogen surface protein mediates covalent host binding. *Elife* **4**, (2015).

54 Echelman, D. J., Lee, A. Q. & Fernandez, J. M. Mechanical forces regulate the reactivity of a thioester bond in a bacterial adhesin. *J Biol Chem* **292**, 8988-8997, (2017).